Title

Dendrite injury triggers neuroprotection in Drosophila models of neurodegenerative disease

Journal

Scientific Reports, 14(1)

ISSN

2045-2322

Authors

Prange, Sydney E

Bhakta, Isha N

Sysoeva, Daria

et al.

Publication Date

2024-10-01

DOI

10.1038/s41598-024-74670-4

Peer reviewed

scientific reports

Check for updates

OPEN

Dendrite injury triggers neuroprotection in *Drosophila* models of neurodegenerative disease

Sydney E. Prange[1,3], Isha N. Bhakta[1], Daria Sysoeva[1], Grace E. Jean[1], Anjali Madisetti[1], Hieu H. N. Le[1], Ly U. Duong[1], Patrick T. Hwu[1], Jaela G. Melton[2] & Katherine L. Thompson-Peer[1,2,3,4]✉

Dendrite defects and loss are early cellular alterations observed across neurodegenerative diseases that play a role in early disease pathogenesis. Dendrite degeneration can be modeled by expressing pathogenic polyglutamine disease transgenes in *Drosophila* neurons in vivo. Here, we show that we can protect against dendrite loss in neurons modeling neurodegenerative polyglutamine diseases through injury to a single primary dendrite branch. We find that this neuroprotection is specific to injury-induced activation of dendrite regeneration: neither injury to the axon nor injury just to surrounding tissues induces this response. We show that the mechanism of this regenerative response is stabilization of the actin (but not microtubule) cytoskeleton. We also demonstrate that this regenerative response may extend to other neurodegenerative diseases. Together, we provide evidence that activating dendrite regeneration pathways has the potential to slow–or even reverse–dendrite loss in neurodegenerative disease.

Keywords Dendrite injury, Axon injury, Regeneration, Neurodegenerative disease, Neuroprotection, *Drosophila*

Neurons are the fundamental units of the nervous system and are responsible for receiving and transmitting information throughout the body. To perform this critical function, neurons use dendrites to receive information from the environment and other neurons and use axons to send information. Across many neurodegenerative diseases, including Huntington's disease (HD), amyotrophic lateral sclerosis (ALS), Alzheimer's disease (AD), Parkinson's disease (PD), and spinocerebellar ataxias (SCAs), neurons exhibit a number of dendrite defects, including dendrite branch loss, branch thinning, branch shortening, and spine loss during early disease stages that are likely detrimental for neuronal function[1–8]. Dendrite defects are evident across neurodegenerative diseases in postmortem patient tissue, but these defects likely appear earlier[9–16]. For example, in HD mice models, dendritic alterations are observed in pre-symptomatic and symptomatic mice before neuronal death[4,17,18]. Similarly, in mouse models of ALS, pathological dendrite changes occur before motor deficits in some neuron types and in early or mid-disease stages in other neuron types[3,19–21]. Because these dendrite defects happen in early disease stages, sometimes pre-symptomatically in animal models, and also appear long before any mass neuronal death associated with late stages of disease, dendrite defects have emerged as a significant contributor to early disease pathogenesis[6,22]. Dendrite defects are therefore a crucial neuronal alteration preceding cell death that may contribute to the initiation of symptoms in the early stages of neurodegenerative disease. Ameliorating these dendrite defects may provide an opportunity for early intervention and disease-modifying therapies in these conditions.

Dendrites are lost in neurodegenerative disease, but neurons have the capacity to regenerate dendrites. Following severing of all dendrite branches, neurons in the *Drosophila* peripheral nervous system (PNS) regenerate the same number of dendrites that an age-matched uninjured neuron has at that developmental time point[23–25]. Dendrites can regenerate in the adult *Drosophila PNS*—even in aged adults[26]. A recent study in mice also showed that neurons regenerate dendrites following initial degeneration after brachial plexus injury[27]. Neurons can regenerate dendrites in the central nervous system (CNS) too: dendrites of neurons in

[1]Department of Developmental and Cell Biology, University of California Irvine, Irvine, CA, USA. [2]Center for the Neurobiology of Learning and Memory, Irvine, CA, USA. [3]Sue and Bill Gross Stem Cell Research Center, Irvine, CA, USA. [4]Reeve-Irvine Research Center, Irvine, CA, USA. ✉email: ktpeer@uci.edu

the zebrafish spinal cord regenerate after dendrite injury[28]. Although mammalian CNS regeneration is generally not spontaneous, insulin treatment has been shown to promote dendrite regeneration after axotomy-induced dendritic retraction in mouse retinal ganglion cells[29]. A recent study also found that dendrite arbor damage to pyramidal neurons in a mouse model of stroke is reverted by day 7 after the injury[30]. The capability for neurons to regenerate their dendrites provides a potential avenue to treat neurodegenerative disease pathology by activating regeneration in degenerating neurons.

To investigate dendrite regeneration in neurodegenerative conditions, we use the *Drosophila melanogaster* dendritic arborization (da) neurons as a model system[31]. *Drosophila* have been important for identifying evolutionarily conserved genes and pathways in mammals and for modeling different diseases and have therefore proven an invaluable model to study neurodegenerative disease[32–39]. Among the neurodegenerative diseases that have been modeled in *Drosophila*, polyglutamine (polyQ) diseases have been modeled extensively.

Polyglutamine diseases are a group of 9 known inherited autosomal dominant neurodegenerative disorders caused by expanded polyglutamine (CAG) repeats in a particular gene and include HD, SCAs, and spinal and bulbar muscular atrophy (SBMA). Short polyglutamine stretches, often 20 or fewer, occur naturally, but their expansion past a certain point, such as 30 or more, in genes related to these disorders leads to pathogenesis (though exact numbers vary based on the affected gene)[40]. In *Drosophila*, expression of human genes with expanded polyglutamine repeats recapitulates human disease pathology such as polyglutamine aggregates, neurodegeneration, dendrite defects, cytoskeletal aberrations, cell type-specific toxicity, behavioral defects, and RNA toxicity[41–51]. In this paper we use *Drosophila* models for SCA1, SCA2, SCA3 and HD to study regeneration in the context of neurodegenerative disease[41,44,50,52,53].

Here we show that degenerating neurons are capable of dendrite regeneration. We further show that injury to a single primary dendrite branch of neurons modeling neurodegenerative diseases induces a neuroprotective response in the rest of the dendrite arbor. Our work demonstrates that this effect is mechanistically tied to stabilization of the actin (but not microtubule) cytoskeleton. We show that this response is specific to dendrite injury, as axon injury and general injury to the surrounding tissue do not induce the same neuroprotection. Our results suggest that triggering dendrite regeneration can potentially act to ameliorate dendrite loss caused by neurodegeneration and further reveals key differences between dendrite and axon regeneration mechanisms.

Results

Class IV da neurons overexpressing pathogenic polyglutamine transgenes experience progressive dendrite degeneration

We began by identifying neurodegenerative diseases where the dendrite degeneration can be readily studied. We can easily observe the dendrite arbors of the da neurons of the *Drosophila* PNS in intact animals. We first sought to characterize the effects of expressing different human polyglutamine (polyQ) transgenes in the highly branched class IV da neurons (ddaC), the less complex class III da neurons (ddaA), and the very simple class I da neurons (ddaE) of the *Drosophila* PNS in intact animals. In agreement with previous results[45], we found that expression of expanded polyglutamine disease transgenes MJD.78Q and ATX1.82Q in class 1 da neurons caused no obvious differences in dendrite arbors in mid 3rd instar larva (Fig. S2A), but did cause dendrite defects in class IV da neurons (see below). We also found that overexpression of MJD.78Q, but not ATX1.82Q, caused defects in both length and branch number in class III ddaA neurons (Fig. S2B-D). We decided to focus on class IV ddaC neurons for our study because defects were observed with multiple pathogenic disease-associated proteins.

We expressed expanded polyQ transgenes modeling spinocerebellar ataxia type 1 (SCA1, ATX1.82Q), spinocerebellar ataxia type 2 (SCA2, ATX2.64Q), spinocerebellar ataxia type 3 (SCA3, MJD.78Q), and Huntington's disease (HD, HTT231NT.128Q) in class IV da neurons[41,44,50,52,53]. In addition to these expanded pathogenic polyQ transgenes with long glutamine repeats, we have non-pathogenic transgenes with short polyQ repeats (ATX1.30Q; ATX2.22Q; MJD.27Q)[44,54,55]. We compare these across time, from 24 h after egg laying (AEL) (earliest 1st instar, larva that just finished embryonic development) to 168 h AEL (latest 3rd instar, larva nearing pupation), and to control neurons.

Wild type (WT) neurons add dendrite branches and dendrite length as well as increase in arbor complexity throughout larval development (Fig. 1A–C and Fig. S1A,C,D,E). Expression of short non-pathogenic polyQ transgenes caused mild dendrite defects or developed similarly to WT and did not degenerate (Fig. 1B). We found that class IV ddaC neurons expressing any of the four long polyQ transgenes initially develop dendrites normally, but then later degenerate, losing dendrite branches and, in most cases, dendrite length. At 24 h AEL, neurons overexpressing expanded polyglutamine disease transgenes were indistinguishable by eye from WT neurons and did not have significantly different dendrite branch number or length (Fig. 1B and Fig. S1A,F). Significant defects in dendrite arbor complexity measured by Sholl analysis in polyQ neurons compared to WT neurons were first observed at 72 h AEL and significant defects in counting branch number and measuring total dendrite length were first observed at 96 h AEL (Fig. 1B,C and Fig. S1C,D,F). Not only are they different from wild type, but all models of polyglutamine disease exhibited the progressive loss of existing dendrites. In other words, we observe not just a slowing in dendrite addition, or just a stabilization of existing branches, but rather a decrease in total branch number over time. We quantified this true dendrite degeneration as a starting branch number at 24 h AEL, a peak at some point (dendrite branch number peaks at 72–144 h AEL, depending on the transgene), followed by a significant decrease in branch number by the last time point at 168 h AEL (Fig. S1E). All polyglutamine disease models also lost total dendrite length after a peak, except for ATX2.64Q. Expression of these constructs also caused degeneration of the axon terminals in the larval ventral nerve cord (Fig. S1B).

While all four polyglutamine disease transgenes cause dendrite loss, there are some differences between the transgenes. MJD.78Q and ATX2.64Q cause dendrite loss at earlier stages (decreasing dendrite number beginning after 72–96 h AEL), while ATX1.82Q and HTT231NT.128Q only begin to decrease dendrite number in older

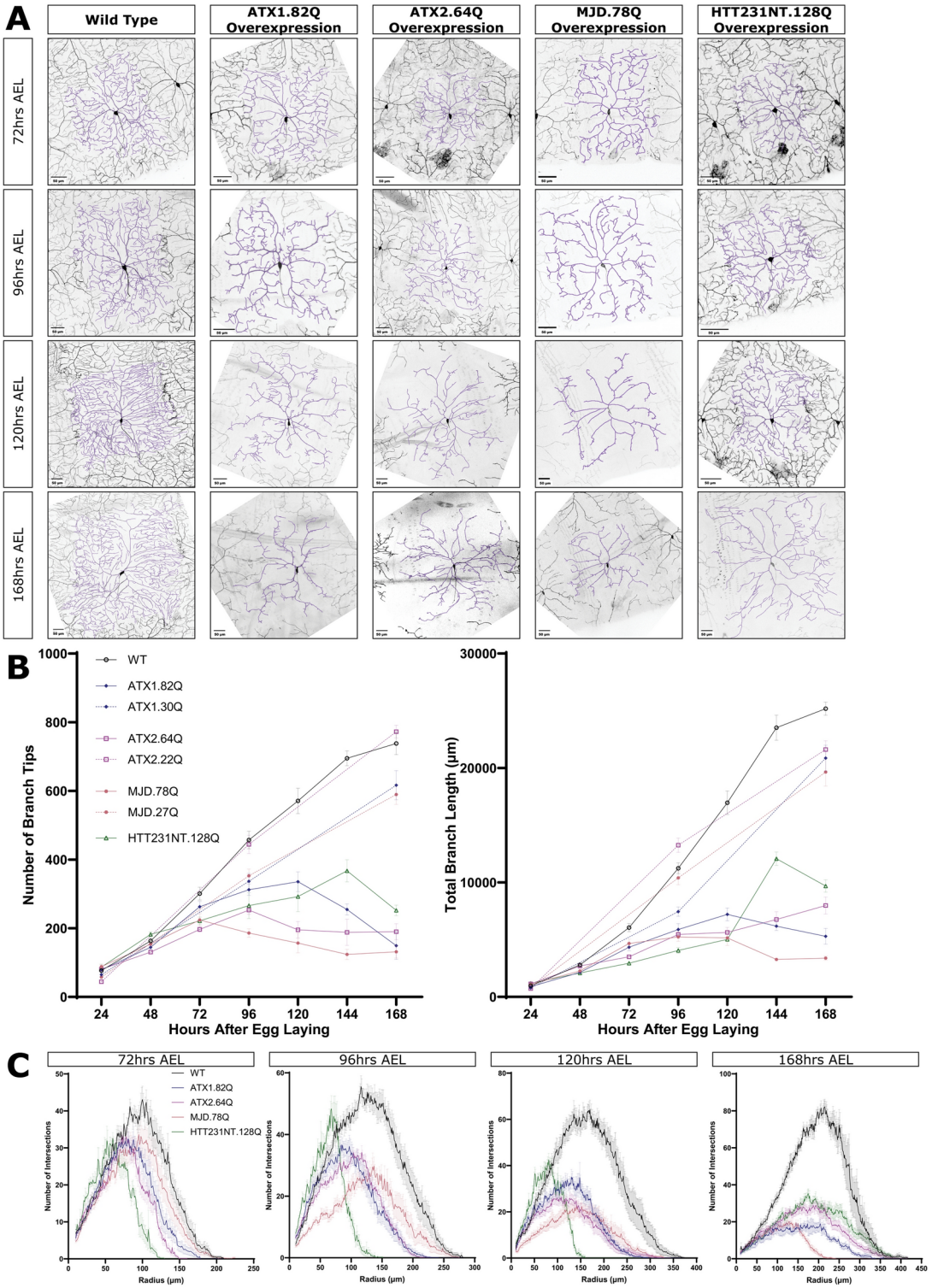

Fig. 1. Overexpressing pathogenic polyQ proteins causes progressive degeneration of dendrites in class IV neurons. (**A**) WT neurons and neurons overexpressing ATX1.82Q, ATX2.64Q, MJD.78Q, and HTT231NT.128Q at 72, 96, 120, and 168 h AEL. Scale bar 50 µm. (**B**) Number of branches (top) and total branch length (bottom) at 24–168 h AEL for WT neurons and neurons overexpressing ATX1.82Q, ATX1.30Q, ATX2.64Q, ATX2.22Q, MJD.78Q, MJD.27Q, and HTT231NT.128Q. Mean ± SEM. (**C**) Sholl analysis profiles at 72, 96, 120, and 168 h AEL for WT neurons and neurons overexpressing ATX1.82Q, ATX2.64Q, MJD.78Q, and HTT231NT.128Q. Mean ± SEM. Legends apply for all graphs in a panel. See also Fig S1, S2.

animals (decreasing dendrite number beginning after 120–144 h AEL). Unlike the other three transgenes, ATX2.64Q overexpression does not cause shortening of dendrite length, though it does decrease dendrite number. Sholl analysis of dendrite arbor complexity seems to be the most sensitive method of quantification, detecting subtle defects at most or all time points, while dendrite branch number and dendrite length changes require a more obvious phenotype. Across all our quantification metrics, HTT231NT.128Q overexpression causes the mildest degeneration, MJD.78Q overexpression causes the most severe degeneration, and ATX1.82Q and ATX2.64Q overexpression each cause moderate degeneration.

Interestingly, although polyQ neurons were mostly indistinguishable from WT at 24 h AEL, a transient increased arbor complexity was observed by Sholl analysis for ATX2.64Q and HTT231NT.128Q neurons that goes away by 48 h AEL (Fig. S1C,D). These results are consistent with emerging evidence that neurodegenerative polyglutamine diseases may have neurodevelopmental components including alterations in dendrite development[56–62].

Overall, while WT ddaC neurons (and neurons expressing short non-pathogenic polyglutamine proteins) grow as larvae develop, ddaC neurons overexpressing pathogenic long polyglutamine proteins grow new dendrite branches and length until a point where they begin to degenerate dendrites and arbor complexity. Although the rate of degeneration differs between transgenes, these results indicate that polyglutamine model neurons allow us to study how neurodegenerative dendrite loss is affected by regeneration following dendrite injury.

Neurons overexpressing pathogenic polyglutamine proteins can regenerate dendrites following severe injury

Previous work in da neurons demonstrated that class IV ddaC neurons can regenerate branch number but not branch length within 72 h after severe injury when all dendrites are severed at 48 h after egg laying[23]. We investigated whether neurons overexpressing polyglutamine disease transgenes were capable of regenerating dendrites after injury. To do this we balded neurons in young larvae (48 h AEL), tracked regeneration from 24 to 72 h after injury, and compared to age-matched uninjured control neurons.

As expected, WT neurons where all branches were severed (balded) at 48 h AEL were able to regenerate dendrite branches between 24 and 72 h after injury (Fig. 2B–D). In the absence of injury, MJD.78Q neurons lose branches and uninjured ATX1.82Q neurons stagnate during this same time (Fig. 2A,C). We found that, surprisingly, overexpression of ATX1.82Q and MJD.78Q did not preclude neurons from regenerating dendrite branches after balding during the same period, and balded ATX1.82Q and MJD.78Q neurons added branch number and length (Fig. 2A,C). The quality of regeneration depended on the transgene. Neurons overexpressing MJD.78Q could regenerate both dendrite branch number and total branch length enough to match uninjured age matched control neurons by 72 h after injury (Fig. 2D). Neurons overexpressing ATX1.82Q were able to regenerate, but not enough to match uninjured age matched controls in branch number or length (Fig. 2D). We also observed regeneration after balding at 48 h AEL for HTT231NT.128Q neurons (Fig. S3). Following full balding in older animals, at 96 h AEL, ATX1.82Q neurons were capable of mild regeneration though MJD.78Q neurons were not (Fig. S3B). These results demonstrate that polyQ model neurons are capable of regenerating dendrites following full balding injury at 48 h AEL and that degeneration does not completely prevent dendrites from regenerating at 96 h AEL. These results suggest that dendrite *de*generation caused by polyglutamine disease transgene expression does not inhibit dendrite *re*generation pathways.

Injury to a single dendrite branch induces neuroprotection in neurons overexpressing pathogenic polyglutamine proteins

Having established that neurons overexpressing expanded polyglutamine disease transgenes are capable of regenerating dendrites, we sought to understand if this regenerative capacity can rescue degeneration at later developmental time points. To assess this, we injured neurons at a time point when polyQ model neurons had significantly fewer dendrite branches and shorter length compared to WT, around 96 h AEL, which marked the start of the degenerative phase of neuron growth (as demonstrated previously, in Fig. 1 and Fig. S1). To determine if dendrite regeneration could alter this degenerative fate, we performed single primary dendrite branch injuries (SBI) to neurons and compared them to age-matched normalized control neurons (NC). Normalized controls were quantified to normalize for the loss of one primary branch by not including that primary branch and its higher order branches in the quantification (Fig. 3A).

We found that single branch injured WT neurons had significantly more dendrite branches and branch length than WT normalized control neurons at 72 h after injury (Fig. 3C). Both single branch injured WT neurons and normalized control WT neurons had significant increases in branch number and length between 24 and 72 h after injury (Fig. 3D). When we determined the amount of branches or length added between 24 to 72 h after injury compared to the starting number of branches at 24 h after injury, there was no significant difference in either percent branches added or percent length added between single branch injured and normalized control WT neurons, indicating that growth in single branch injured neurons was proportional to the number of branches and length the neurons started with after injury (Fig. 3C). In other words, the growth in WT single branch injured neurons was equivalent to developmental growth of age-matched control neurons during the same time.

Next, we examined the response of pathogenic long polyQ neurons to single branch injury, compared to normalized controls. We first looked at the terminal time point, 72 h after injury. All single branch injured polyQ model neurons had significantly more dendrite branches and length at 72 h after injury than their corresponding normalized controls (Fig. 3F,I,L,O). We next looked at growth and degeneration during the time between injury and the terminal time point. As discussed above, both single branch injured and normalized control WT neurons added branches proportionally to their starting branches (Fig. 3D). In contrast, all single branch injured polyQ model neurons added more branches proportional to their starting branches than corresponding

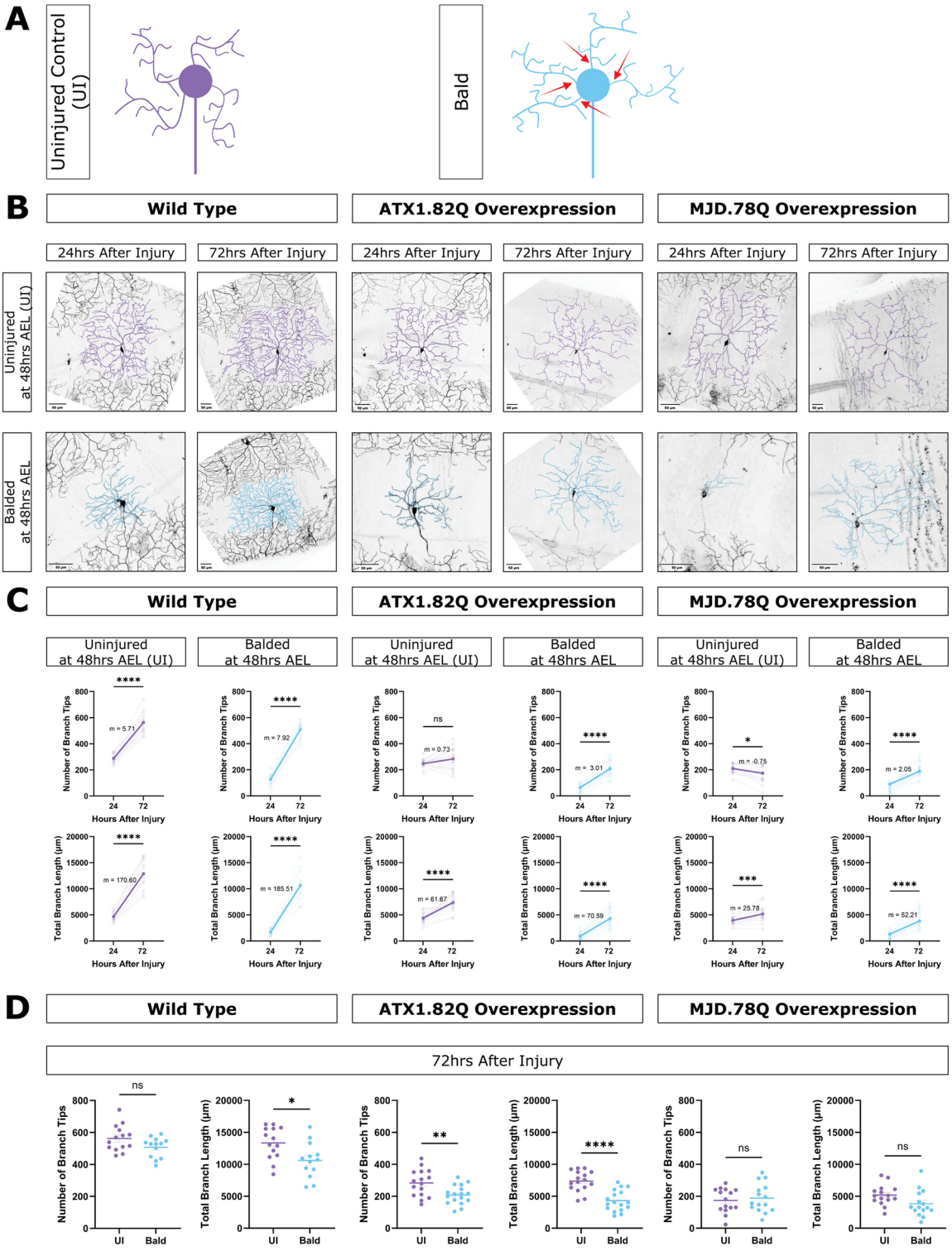

Fig. 2. Neurons overexpressing pathogenic polyQ proteins can regenerate dendrite arbors following complete removal at 48 h AEL. (**A**) Schematic of uninjured neurons (purple) and bald neurons (blue). Red arrows represent 2 photon laser injury. (**B**) Uninjured neurons and balded neurons for WT, ATX1.82 overexpression, and MJD.78Q overexpression neurons at 24 and 72 h after injury done at 48 h AEL. Scale bar 50 µm. (**C**) Number of branch tips (top) and total branch length (bottom) at 24 and 72 h after injury for uninjured (purple) and balded (blue) for WT, ATX1.82Q, and MJD.78Q overexpression neurons. Individual neurons (faded) and mean (bold) values shown, with slope (m) between the mean 24 and 72 h after injury values. Paired t-test. (**D**) Number of branch tips (left) and total branch length (right) between uninjured and balded WT, ATX1.82Q, and MJD.78Q overexpression neurons at 72 h after injury. Welch's t-test. See also Fig S3.

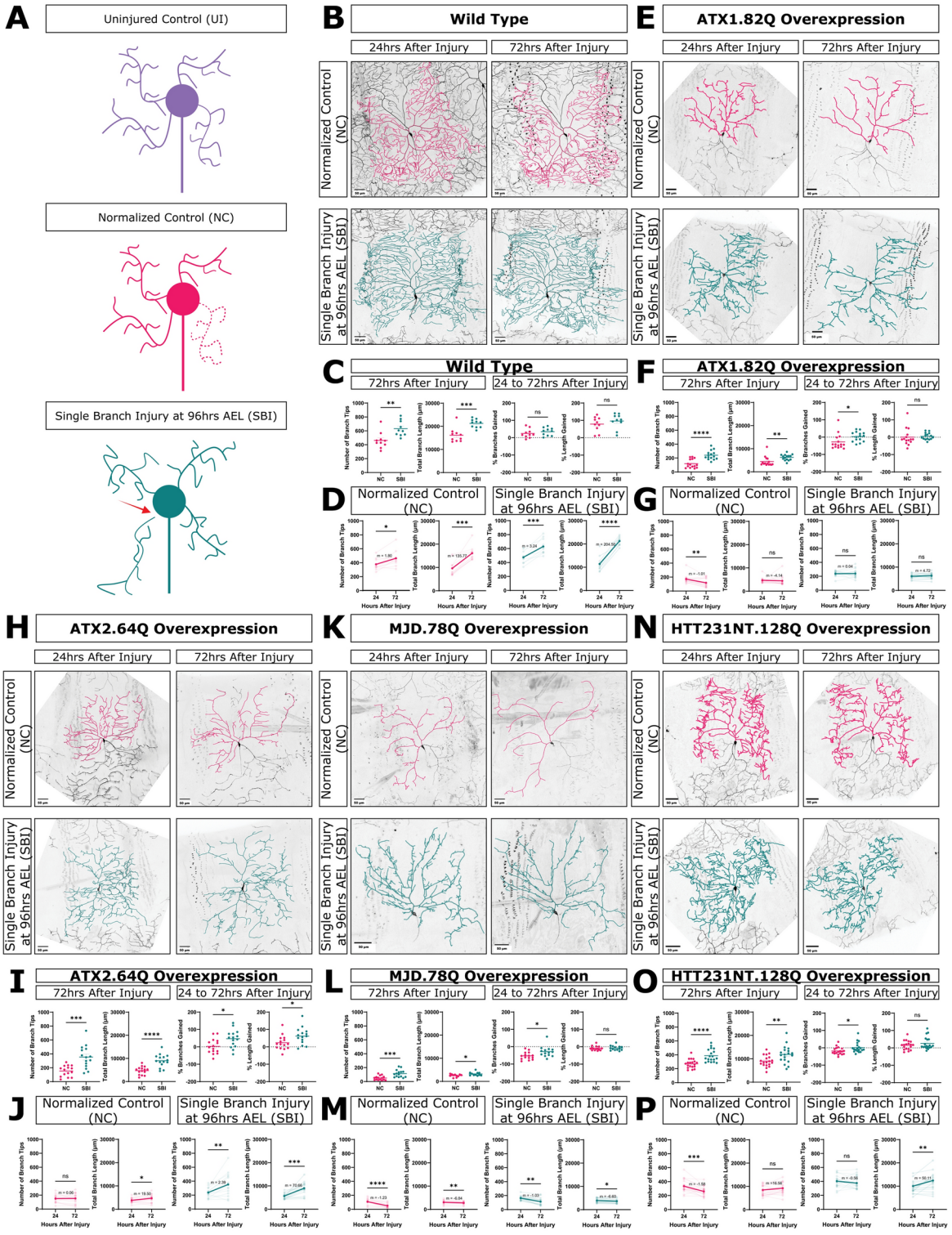

Fig. 3. Injury to a single dendrite branch induces neuroprotection in neurons overexpressing pathogenic polyQ proteins. (**A**) Schematic of uninjured neurons (purple, UI), normalized control neurons (pink, NC), and single branch injured neurons (green, SBI). The red arrow represents 2 photon laser injury. (**B**, **E**, **H**, **K**, **N**) Normalized control and single branch injured neurons at 24 and 72 h after injury for WT and ATX1.82Q, ATX2.64Q, MJD.78Q, and HTT23NT.128Q overexpression neurons. Scale bar 50 µm. (**C**, **F**, **I**, **L**, **O**) Comparing number of branch tips and total branch length of NC and SBI neurons at 72 h after injury, or comparing % change in number of branch tips and total branch length between 24 to 72 h after injury between NC and SBI neurons. Welch's t-test. (**D**, **G**, **J**, **M**, **P**) Number of branch tips and total branch length at 24 and 72 h after injury for NC (pink) and SBI (green) neurons. Individual neurons are faded, solid lines represent the average slope (m) between the mean 24 and 72 h after injury values. Paired t-test. See also Fig S4–S8.

normalized controls (Fig. 3E,I,L,O). This trend was also true for added length in the case of single branch injured ATX2.64Q neurons (Fig. 3I). This indicates that, unlike in WT neurons, the growth experienced by single branch injured polyQ neurons was different from the stagnation or degeneration seen in age-matched control neurons. Additionally, we observed that location of the injured branch did not affect the location of new growth in the rest of the arbor (Fig. S5).

The effect of single branch injury on the rate of branch number change and length change during this time differed depending on the transgene. For ATX1.82Q and HTT231NT.128Q neurons, we observed that single branch injury rescued the significant decrease in branch number seen in ATX1.82Q and HTT231NT.128Q normalized control neurons, inducing branch number stagnation rather than branch loss during that time (Fig. 3G,N). For ATX2.64Q neurons, single branch injury induced a significant increase in branch number compared to stagnation for normalized control neurons (Fig. 3J). The effect of single branch injury on MJD.78Q neurons was weaker, with both single branch injured and normalized control neurons decreasing in both branch number and length, though at a slower rate for the single branch injured neurons (Fig. 3M). Overall, we observed that single branch injury was able to alter, and in some cases rescue, the dendrite loss trajectory of pathogenic polyQ neurons between 24 and 72 h after injury.

To determine whether this was specific to degenerating polyQ neurons, we also examined responses to single branch injury in three non-pathogenic short polyQ overexpression models, ATX1.30Q, ATX2.22Q, and MJD.27Q. We found that ATX1.30Q and ATX2.22Q neurons appeared like WT in the uninjured condition and in response to single branch injury (Fig. S6D-G). We also found that MJD.27Q neurons exhibited variable degeneration at late time points but responded to single branch injury similarly to WT neurons (Fig. S6A–C). Overall, this suggested that the injury-induced protection was specific to pathogenic polyQ neurons, and not observed when non-pathogenic short polyQ proteins were expressed.

We also examined response to single branch injury in a non-polyQ-induced model of dendrite degeneration by overexpressing a transgene for the 0N3R isoform of human tau (MAPT)[63] in class IV neurons and conducting single branch injuries at 96 h AEL. We found that single branch injured hMAPT.0N3R overexpression neurons also had significantly more dendrite branches and length than normalized controls and added more branches and length proportionally than normalized controls (Fig. S7B). We also found that while normalized control hMAPT.03NR neurons have a slightly negative but nonsignificant decrease in branches between 24 and 72 h after injury, single branch injury was able to rescue this to significantly positive branch growth during this same time (Fig. S7C). These results suggest that the single branch injury-induced neuroprotection may be applicable in other models of neurodegenerative disease. We further examined single branch injury in MJD.78Q class III ddaA neurons, the only model where degeneration was observed in class III neurons, and found that single branch injury induced recovery of branch length but not branch number (Figure S8).

Altogether, we observed that single branch injury induces regenerative growth that increased dendrite number and length in pathogenic polyQ model neurons and that these findings extend to non-polyQ models of neurodegeneration and other neuron types. Although there were differences between individual transgenes, single branch injury activated regeneration across all polyQ models we tested, leading to protection of existing branches or growth of new branches. This supports the idea that injury of one dendrite branch can effectively "turn on" regenerative processes in uninjured branches, to slow or limit their degeneration. We refer to this phenomenon as single branch injury induced neuroprotection.

Axotomy does not induce neuroprotection in neurons overexpressing pathogenic polyglutamine proteins

We next tested if the neuroprotection was specific to dendrite injury by instead injuring axons (axotomy). To assess this, we performed axotomies at ~ 40 µm from the cell body at 96 h AEL and assessed dendrite architecture at 24 and 72 h after injury. We performed axotomies at this distance to avoid dendrite-to-axon transition during axon regeneration[64–66]. WT neurons lost dendrite branches and length following axotomy, and axotomized neurons had significantly fewer dendrite branches and length than age-matched uninjured control neurons at 24 h after injury (Fig. 4B,C and Fig. S9A). This is in agreement with previous observations in our system and other species[54–58]. Axotomized WT neurons lost branches and length between 24 and 72 h after injury while uninjured age-matched control WT neurons grew branches and length during that time (Fig. S9A).

We found that axotomy of neurons overexpressing ATX1.82Q and MJD.78Q did not produce any neuroprotection (Fig. 4B,C). Like their uninjured controls, axotomized ATX1.82Q neurons and axotomized MJD.78Q neurons both lost branches and length between 24 and 72 h after injury (Fig. S9B,C). This shows that axon injury does not activate a neuroprotective effect in degenerating polyQ neurons, unlike what was observed with dendrite branch injury, establishing the neuroprotective effect as specific to dendrite injury.

Injury-induced neuroprotection is specific to primary branch injury and is cell autonomous

Having established that only dendrite injury activates a neuroprotective effect, we also tested whether a small injury to a terminal dendrite branch could recapitulate the effect of a single primary dendrite branch injury. For WT neurons, we did not observe a significant difference in branch number or length between uninjured age-matched control neurons and terminal branch injured neurons at 72 h after injury (Fig. 4D,E). Similarly, for both ATX1.82Q and MJD.78Q, terminal branch injury was not sufficient to induce the neuroprotective effect seen with single primary branch injury (Fig. 4D,E). Overall, terminal branch injury was not sufficient to induce growth for WT neurons or neuroprotection for polyQ neurons.

To test if the observed neuroprotective effect was cell autonomous, or perhaps a result of injuring surrounding cells such as epidermal cells, we also conducted experiments where the laser was aimed at a space near a primary dendrite branch at a similar distance from the cell body as single branch injury experiments. In WT neurons, neurons that were exposed to a near-miss injury were not significantly different in branch number or length

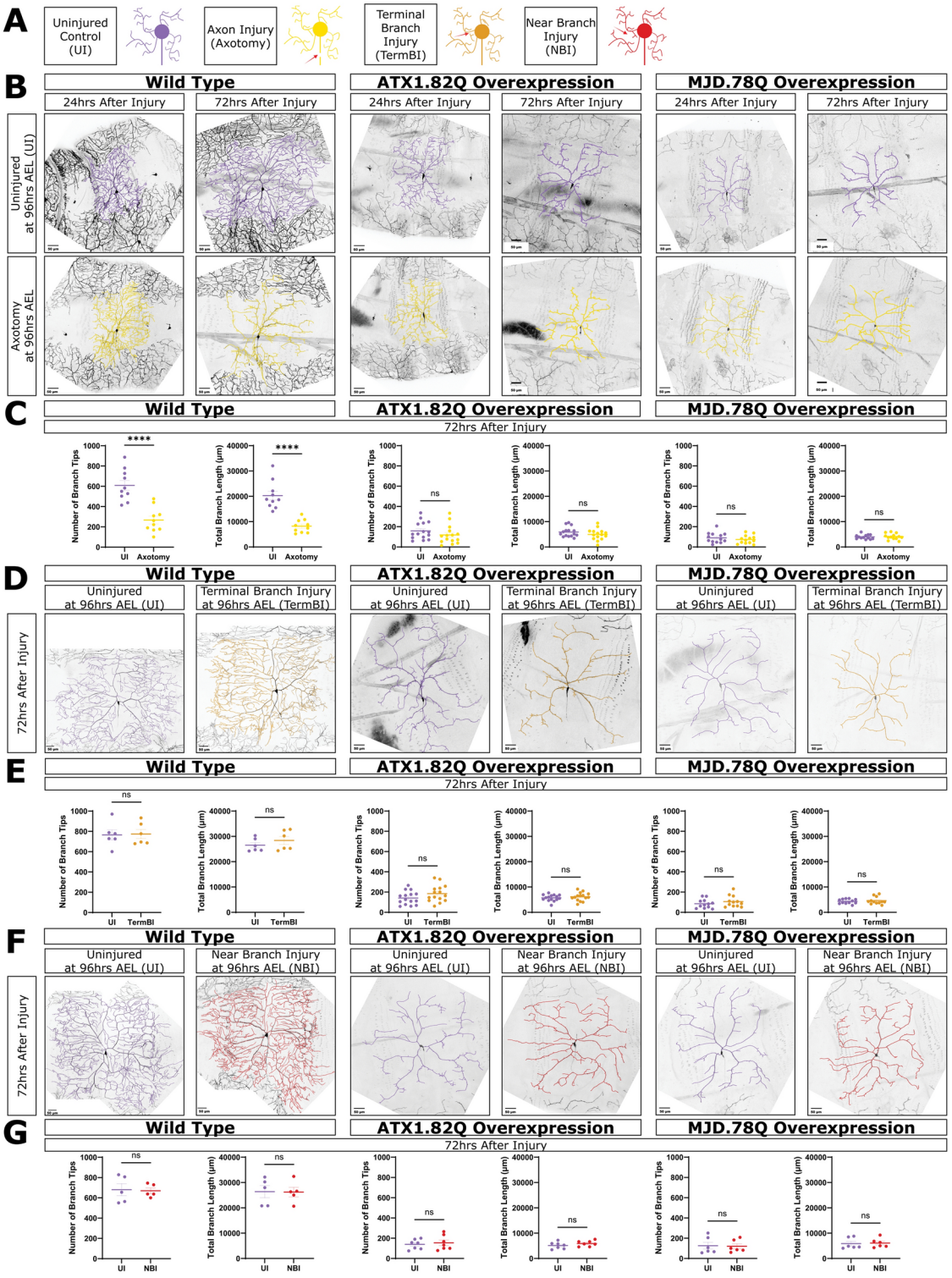

Fig. 4. Axotomy, terminal branch injury, and near branch injury do not induce neuroprotection. (**A**) Schematic of uninjured neurons (purple, UI), axotomized neurons (yellow), terminal branch injured neurons (orange, TermBI), and neurons left uninjured but exposed to an injury near a dendrite branch (red, NBI). Red arrows represent 2 photon laser injury. (**B**) Uninjured and axotomized WT, ATX1.82Q, and MJD.78Q overexpression neurons at 24 and 72 h after injury. Scale bar 50 μm. (**C**) Number of branch tips and total branch length between UI and axotomy at 72 h after injury. Welch's t-test. (**D**) Uninjured and terminal branch injured neurons at 72 h after injury. Scale bar 50 μm. (**E**) Number of branch tips and total branch length between UI and TermBI at 72 h after injury. Welch's t-test. (**F**) Uninjured and uninjured but exposed to a near branch injury neurons at 72 h after injury. Scale bar 50 μm. (**G**) Number of branch tips and total branch length between UI and NBI at 72 h after injury. Welch's t-test. See also Fig S9.

at 72 h after injury from age-matched uninjured neurons with no laser injury at all (Fig. 4F,G). Similarly, a near-miss injury did not produce a similar neuroprotective effect in either ATX1.82Q or MJD.78Q neurons (Fig. 4F,G). These data suggest that the single primary dendrite injury induced neuroprotection we observed is due to processes being initiated inside the injured cell, leading to growth and retention of branches, rather than a result of surrounding cells.

Single branch injury, but not axotomy, induces stabilization of the actin, but not the microtubule, cytoskeleton

We next wanted to determine a mechanistic explanation for the single branch injury-induced regenerative neuroprotection we observed in polyQ neurons, so we looked at microtubules (MT) and F-actin in these neurons after injury. We hypothesized that single branch injury-induced regeneration might be triggering stabilization or rescue of actin and MTs in degenerating polyQ neurons, leading to neuroprotection.

First, we looked at actin in the neurons. To look at F-actin in these neurons, we chose to use the construct GMA, a fusion protein which consists of GFP fused to the cytoskeletal linker protein moesin's actin-binding domain, that directly labels F-actin during nucleation[67–69]. This construct shows areas with stable actin and was expressed only in the class IV da neurons. To determine if F-actin stabilization might play a role in the single branch injury-induced neuroprotective response that we observed, we injured neurons and quantified the GMA signal in the cell body and dendrite branches at 24 h after injury.

In WT neurons, we found that single branch injury did not change stable F-actin in either the cell body or dendrite branches, and that axotomy significantly reduced F-actin levels in both the cell body and dendrite branches (Fig. 5A,B). In contrast, for ATX1.82Q, ATX2.64Q, and HTT231NT.128Q neurons, single branch injury caused an increase in F-actin in the cell body and dendrite branches (Fig. 5A,B). Axotomy, however, reduced F-actin in the cell body of ATX2.64Q and HTT231NT.128Q neurons and did not change F-actin in ATX1.82Q neurons (Fig. 5A,B). Axotomy did not change F-actin in branches in ATX1.82Q, ATX2.64Q, and HTT231NT.128Q neurons (Fig. 5A,B). In addition, no significant F-actin changes were observed in non-pathogenic and non-degenerating ATX1.30Q or ATX2.22Q neurons after single branch injury, indicating that the increase following single branch injury was not caused by presence of a polyglutamine transgene and seems to be specific to degenerating neurons following single branch injury (Fig. S5E). These results show that single branch injury triggers stabilization of F-actin in both dendrite branches and in the cell body for degenerating neurons, while axotomy does not. Our results show that axon injury leads to loss of F-actin in the cell body and dendrites whereas dendrite injury leads to an increase in F-actin in both the cell body and dendrites, but this is only seen in neurons already defective for F-actin, such as polyQ model neurons. These data suggests that single branch injury causes regenerative neuroprotection in degenerating neurons by leading to stabilization of the actin cytoskeleton and that this does not occur following axotomy.

Next, we wanted to determine if the neuroprotective mechanism was specific to actin stabilization or if it also involved changes in MT stability and dynamics. We examined microtubules using three different approaches: visualizing Tau-GFP, immunostaining for futsch/MAP1b, and observing new MT growth using EB1-GFP comets. We first looked at stable microtubule bundles using the construct Tau-GFP, which labels endogenous microtubules in both axons and dendrites of all da neurons[70–72]. We injured and subsequently imaged neurons with ppk-CD4-tdTomato and used Tau-GFP to visualize microtubules 24 h after injury. We found that single branch injury did not change the amount of Tau-GFP in either dendrites or the cell body for WT or polyQ model neurons (Fig. 5C,D). We next immunostained for *Drosophila* microtubule associated protein futsch/MAP1b at 24 h after injury and did not see an effect on microtubule localization or density (Fig. S5F). Finally, we examined microtubule dynamics by imaging EB-1 comets in neurons 24 h after injury. Interestingly, single branch injury induced mixed microtubule polarity in both WT and polyQ neurons (Fig. S5D). In addition, single branch injury rescued the significantly increased microtubule dynamics caused by MJD.78Q overexpression (Fig. S5C). However, the same was not observed for ATX1.82Q neurons where single branch injury did not affect comet number or velocity (Fig. S5B). This indicated that, although single branch injury did induce some changes in microtubule dynamics, new microtubule formation or microtubule stabilization likely do not contribute to a core mechanism behind the observed neuroprotection.

Together these data suggest that the mechanism of single branch injury-induced neuroprotection is likely stabilization of F-actin. Our observations also suggest that actin stabilization occurs early in the regenerative process after injury and this early stabilization is enough to stabilize the arbor for sustained neuroprotection we observed later at 72 h after injury.

Discussion

Our study presents the first evidence that dendrite regeneration is possible in degenerating neurons and demonstrates that dendrite regeneration triggered by single branch injury can induce neuroprotection of the remaining dendrite arbor in ddaC neurons modeling neurodegenerative diseases. We demonstrate that this effect is cell autonomous and specific to primary dendrite branch injury—not axon injury. Our results also show that this neuroprotection is supported by the mechanism of early stabilization of the actin cytoskeleton in both dendrite branches and the cell body. Our results are summarized in Fig. S11.

Neurodegeneration does not prevent regeneration

Dendrite degeneration is a hallmark of human neurodegenerative disease that was first identified in early studies of postmortem patient brain tissue and further established as an early cellular alteration linked to functional and behavioral deficits by subsequent work in animal models[1,2,4–16,19,22]. Recovery of these dendrites in affected neurons would require regenerative mechanisms being unimpeded by neurodegeneration. Our work demonstrates that although neurodegeneration leads to progressive dendrite loss, it does not prevent dendrite

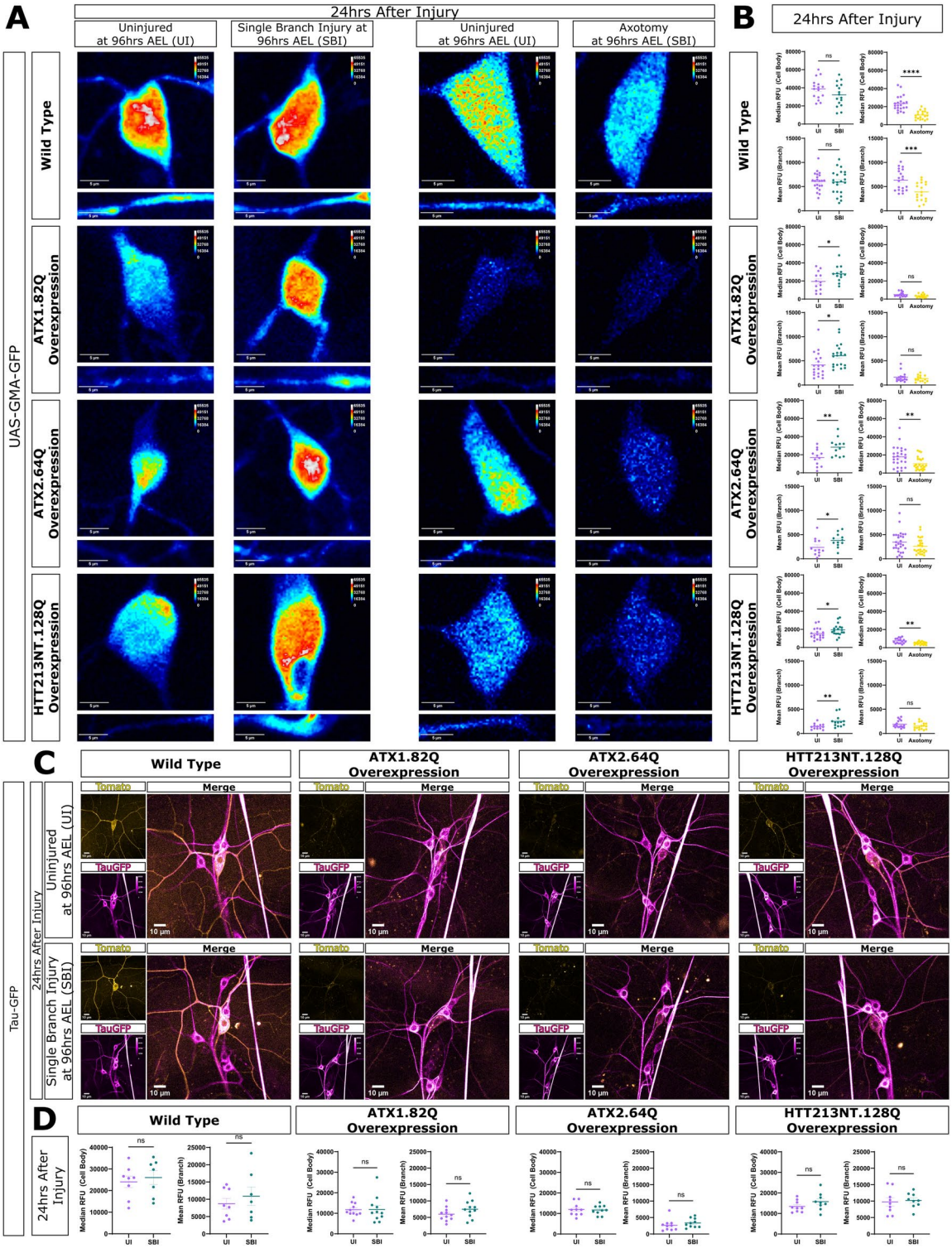

Fig. 5. Single branch injury, but not axotomy, induces stabilization of the actin, but not the microtubule, cytoskeleton. (**A**) GMA imaging at 24 h after injury for WT, ATX1.82Q, ATX2.64Q, and HTT231NT.128Q neurons. Images (L > R): uninjured control cell body (top) and branch (bottom) images for SBI experiments, SBI cell body and branch, uninjured control for axotomy experiments, axotomy cell body and branch. Scale bar 10 µm. (**B**) Median cell body RFU (top) and mean branch RFU (bottom) between uninjured versus SBI neurons (left) and between uninjured versus axotomy neurons (right) for WT, ATX1.82Q, ATX2.64Q, and HTT231NT.128Q neurons. Welch's t-test. (**C**) TauGFP imaging at 24 h after injury for uninjured, SBI, and axotomy of WT, ATX1.82Q, ATX2.64Q, and HTT231NT.128Q neurons. ppk-CD4-tdTomato pseudo-colored in yellow, Tau-GFP pseudo-colored in magenta. (**D**) Median cell body RFU and mean branch RFU between uninjured versus SBI neurons for WT, ATX1.82Q, ATX2.64Q, and HTT231NT.128Q neurons. Welch's t-test. See also Fig S10.

regeneration. We demonstrate that both neurons destined to degenerate and neurons actively degenerating are capable of some regeneration, with varying success depending on the type of dendrite injury, the stage of degeneration, and the disease model. We further show that this effect not only applies to polyglutamine disease models, but another neurodegenerative model caused by overexpression of human tau. Together, these data suggest that neurons demonstrate capacity to recover from neurodegeneration, that neurodegeneration does not prevent regeneration, and that dendrite degeneration in neurodegenerative disease is reversible.

The cytoskeleton in regeneration and neurodegenerative disease

Proper MT and actin regulation are critical for neurite growth, morphology and stability[45,73]. Enrichment of local F-actin is associated with dendritic branching, and dendritic arbor length is highly interrelated with local MT quality[73]. In addition, the importance of actin nucleator Cobl in mice and the actin regulators RAC GTPase CED-10 and RhoGEF TIAM-1 in *C. elegans* for dendrite regeneration suggests a key role for the actin cytoskeleton in the regeneration process of dendrites[30,74]. Similarly, the MT binding protein Patronin (CAMSAP1/2/3 in mammals) and its microtubule nucleation function have been implicated in dendrite regeneration[75–77]. Our results suggest that stabilization of F-actin plays an important role in the response to dendrite injury and subsequent regeneration. Although single branch injury had variable effects on stable microtubules and dynamics, we found that dendrite injury induced mixed microtubule polarity in all neurons, suggesting that changes in microtubule polarity play a role in response to dendrite injury and dendrite regeneration.

In accordance with the importance of the cytoskeleton for neuron development and stability, cytoskeletal dysregulation is a hallmark of neurodegenerative disease[78–84]. Regulators of the cytoskeleton such as cofilin, RhoA/ROCK pathway components, MAPs, GSK3β have emerged as potential therapeutic targets for treating this dysregulation[81,84–88]. It has previously been shown that F-actin levels are reduced in SCA1 and SCA3 model class IV da neurons[45]. Our results suggest that this reduction can be ameliorated by activating dendrite regeneration mechanisms via single branch injury. This indicates that dendrite regeneration mechanisms present another pathway that may be targeted to modulate the actin cytoskeleton for therapeutic potential in neurodegenerative disease.

Insights about dendrite and axon regeneration

Our work demonstrates a unique phenomenon that can be triggered by dendrite injury and dendrite regeneration mechanisms, but not for axon injury and axon regeneration mechanisms, highlighting the need for more focus on the molecular underpinnings of dendrite regeneration. Much focus has been placed on studying axon injury and regeneration, with little attention paid to dendrite injury and regeneration, and questions remain about how much these two processes share or diverge. Although dendrite and axon regeneration after injury share certain mechanistic aspects, such as regulation by the Akt pathway, other aspects have emerged as unique to one process and not the other[25]. For example, axon regeneration is triggered via a conserved signaling cascade that relies on the dual leucine zipper kinase DLK, but DLK and its downstream transcription factors have also been shown to be dispensable for dendrite regeneration[24,74,89–93]. Similarly, dendrite regeneration in *Drosophila* requires the tyrosine kinase Ror, but this kinase is not required for axon regeneration[77]. Our study adds to this body of evidence by showing that dendrite regeneration mechanisms, and not axon regeneration mechanisms, have unique potential to protect dendrite arbors in degenerating neurons. Our work also demonstrates a notable mechanistic difference between axon and dendrite regeneration. In axotomized neurons, F-actin in the cell body and dendrite arbor is reduced early in the regeneration time frame, while the opposite seems to be triggered following dendrite injury. Although we did not see an increase in F-actin in WT neurons following single branch injury, our results in polyQ model neurons suggests that this increase may only be observable in neurons where F-actin levels are already lowered or dysregulated or that this may be more transient or tightly controlled to maintain equilibrium in WT neurons. Our work along with others demonstrates a growing need for deeper investigation into mechanisms behind dendrite regeneration to both inform our understanding of regenerative processes that may be harnessed in neurons and to elucidate new avenues of exploration in diseases that affect dendrites.

Is dendrite regeneration just upregulation of dendrite maintenance mechanisms?

Another question that remains in the field of dendrite regeneration is whether dendrite regeneration is entirely a result of upregulated dendrite maintenance mechanisms, has some overlap with dendrite maintenance mechanisms, or is its own completely separable process. Although it is known that this regeneration is different from developmental growth of dendrites, it is not understood how much these processes of development versus regeneration overlap and whether something that prevents proper development and maintenance, such as neurodegenerative disease, will also prevent regeneration. Both how dendrites are maintained throughout life and how they can regenerate after injury is largely understudied and little is known about how these two processes may be either interconnected or distinct from one another.

Growing dendrite arbors are dynamic and their continual extension and retraction until they reach maturity is influenced by synaptic connections[94–96]. After development, dendrites and synapses must be actively maintained with long-term stability regulated by a combination of signaling pathways, synaptic inputs, and structural support from the cytoskeleton and cell adhesion and scaffolding molecules[94–96]. Our work suggests that dendrite maintenance and dendrite regeneration are indeed separable processes because defective maintenance does not preclude regeneration or regrowth after injury. We demonstrate that neurons that fail to maintain their dendrite arbors due to neurodegenerative dendrite loss are still capable of regeneration. Although the regeneration process after severe balding injury is stunted in degenerating neurons at later stages of degeneration, we still observed some regrowth. Because defective maintenance in our study is due to neurodegeneration that perturbs many aspects of neuronal homeostasis, health, and maintenance, further exploration looking at dendrite regeneration

in neurons where dendrite maintenance mechanisms are more directly inhibited is needed to distinguish the two processes more definitively.

Beneficial outcomes of stress

Moderate stressors have been associated with benefits for organisms. Previous work by Neumann et al. demonstrated that introducing priming lesions both at the time of spinal cord injury and a week later were able to enhance axonal regeneration in adult rat DRG neurons.[97] Acute stress has also been shown to increase neurogenesis in the adult rat hippocampus, leading to benefits in learning and memory tests[98]. Mild stress due to dietary restriction has shown benefits for lifespan, health span and brain health[99–101]. Our work demonstrates a similar phenomenon in the context of neurodegenerative disease and dendrite repair. Previous work has shown that activating the integrated stress response is beneficial in HD and ALS models[102–105]. In our study, we show that the stress of a subtle injury to a single dendrite can cause a beneficial regenerative response in the remaining arbor. Our work adds to the growing body of evidence that acute minor injury or transient stress can have beneficial outcomes for neuronal repair and health.

Implications for and potential therapeutic avenues in neurodegenerative disease

Our results reveal an unexplored pathway for potential therapeutic targets in neurodegenerative disease. These new findings provide the first evidence for potential regeneration of dendrites lost in neurodegenerative disease. Our work suggests that dendrite regeneration mechanisms can be harnessed to recover and preserve dendrites, potentially delaying or slowing the cellular effects of neurodegenerative disease and ultimately improving neuronal function. Further work to characterize the intermediate factors controlling the neuroprotective response that leads to downstream actin stabilization will be key to discovering new therapeutic targets in neurodegenerative disease. Perhaps if we can modulate these factors similarly but in the absence of direct neuronal injury, we can achieve sustained neuroprotection. These therapeutic targets can be further studied in mouse and human cellular models of neurodegenerative disease for potential therapeutic applications.

Our study also hints that just having the gain of function effect of expanded polyglutamine aggregate overexpression is not only enough to recapitulate neurodegenerative phenotypes, but also transient neurodevelopmental phenotypes. A growing amount of evidence suggests altered neurodevelopment due to loss of function of important genes for brain development like huntingtin is an important feature of disease pathogenesis in polyglutamine diseases and other neurodegenerative disorders[56–62,106–108]. Our study suggests that, in addition to LOF effects, GOF effects may also play a role in neurodevelopmental defects observed in polyglutamine disease.

Conclusions

Taken together, the results of our study support the idea that injury of one dendrite branch can effectively "turn on" regenerative processes in uninjured branches, leading to retention or new growth and slowing or limiting degeneration in spared branches. These results present a promising avenue to explore triggering dendrite regeneration in the absence of injury as a possible treatment for degenerative dendrite loss in neurodegenerative diseases. Future work should focus on assessing these phenomena in adult mature neurons and in neurons of the CNS. Further studies have the potential to elucidate both important mechanisms underlying dendrite regeneration and potential therapeutic targets for intervention in neurodegenerative disease.

Experimental model and subject details

Drosophila strains

Drosophila stocks were maintained at room temperature. Larva for experiments were maintained at room temperature or in an incubator at 22.5 °C and 70% humidity. Both male and female larva were used for all experiments. The following fly strains were used in this study: Canton-S, ppk-CD4-tdGFP (chromosome 3)[109], ppk-GAL4 (chromosome 2)[110], ppk-CD4-tdTomato (chromosome 2)[109], UAS-CD4-tdTomato (chromosome 2)[109], $Gal4^{2-21}$ (chromosome 3)[111], UAS-GMA (BDSC#31776)[112], UAS-EB1-GFP (BDSC#35512)[113], $WeeP^{304}$Tau-GFP) (courtesy of Melissa Rolls)[71], UAS-Hsap\HTT231NT.128Q (courtesy of Juan Botas)[52], UAS-hATXN3.tr-Q78 (BDSC#8150)[41,53], UAS-Hsap\ATX1.82Q (BDSC#33818)[44], UAS-ATXN2-CAG-64 (courtesy of Nancy Bonini)[50], UAS-hATXN3.tr-Q27 (BDSC#8149)[55], UAS-Hsap\ATX1.30Q (BDSC#39739)[44], UAS-ATXN2.22Q (BDSC#79594)[54], GAL-4^{19-12}>CD4-tdGFP (chromosome 3)[114], UAS-hMAPT.03NR (BDSC #93609)[63]. A complete list of fly stocks can be found in the supplementary methods.

Method details

Key resources are listed in the supplemental methods.

Generation of fly lines and experimental crosses

Crosses were performed at room temperature or in an incubator at 22.5 °C and 70% humidity on a plate made of grape juice and agarose (grape plate) with yeast paste to synchronize animal age. Cross progeny larva for experiments were kept on grape plates at room temperature or in an incubator at 22.5 °C and 70% humidity. Assays to assess development, injury, and regeneration in class IV ddaC neurons were performed by crossing fly lines expressing ppk-CD4-tdGFP and ppk-GAL4 with CantonS flies or flies expressing UAS-polyQ. Assays to assess development in class 1 ddaE neurons were performed by crossing fly lines expressing $GAL4^{2-21}$ and UAS-tdTomato with CantonS flies or flies expressing UAS-polyQ. Assays to assess F-actin in class IV ddaC neurons were performed by crossing fly lines expressing UAS-GMA under control of ppk-GAL4 with CantonS (WT) flies or flies expressing UAS-polyQ. Assays to assess microtubule dynamics in class IV ddaC neurons were performed

by crossing fly lines expressing UAS-EB1-GFP under control of ppk-GAL4 with CantonS flies or flies expressing UAS-polyQ. Assays to observe stable microtubule bundles in class IV ddaC neurons were performed by crossing fly lines expressing ppk-gal4, ppk-CD4-tdTomato and WeeP^{304}Tau-GFP with CantonS flies or flies expressing UAS-polyQ. Following injury and subsequent imaging, larva were individually housed on grape plates with yeast paste.

Dendrite and axon injury assays

Imaging, excluding immunohistochemistry, was performed in living whole-mount larvae. For all assays involving injury, dendrites or axons were severed from da neurons by focusing a two-photon 860–900-nm laser mounted on a Zeiss LSM 780 or Zeiss LSM 980 fluorescence microscope on a dendrite using methods described previously[23–25]. To immobilize the larva for injury, larva were mounted on a glass slide between a 4% agarose pad and a coverslip using glycerol as a mounting media. For larger larva, vacuum grease and tape was used to keep the coverslip in place and immobilize the larva. To injure dendrites or axons on the Zeiss LSM 780, neurons were imaged using the 2-photon and cut with the 2-photon by focusing the laser on the desired area until bleaching of the fluorophore signal was seen, indicating a cut. To injure on the Zeiss LSM 980, neurons were imaged using 488 nm or 560 nm green or red lasers and injured using the bleaching function with the 2-photon. Axons were distally severed ~ 40 uM away from the cell body to avoid dendrite-axon conversion[115]. For the balding injury assay, the laser was focused on primary or secondary dendrite branches near the cell body to remove all branches in the fewest cuts possible without damaging the cell body. For the single branch injury assay, the laser was focused on a single primary dendrite branch near the cell body. For the terminal branch injury assay, the laser was focused on a terminal dendrite branch near the cell body. For the near branch injury assay, the laser was focused to a point near a dendrite branch for a comparable amount of time to dendrite injury assays. Neurons were imaged on a Zeiss LSM 700 or Zeiss LSM 980 fluorescence microscope 24 h after injury to confirm successful injury (total dendrite removal and distinct new dendrite arbor for balding injury, single branch removal for single branch injury, terminal branch removal for terminal branch injury, and distal axon removal for axon injury) and, for some experiments, at 72 h after injury to assess regeneration. Successful balding injury was assessed by observing dendrite blebbing immediately after injury, comparing the 24 h after injury images to the before injury images to assess if the arbors look different, and evaluating territory coverage of new arbors at 24 h. Uninjured control neurons were imaged on the day of injury but left alone and then imaged at 24 and 72 h after injury for comparison to injured neurons. All injury assays were performed such that there was sufficient time for regeneration to occur after injury before pupation (at least 72 h).

Immunohistochemistry

Larva were anesthetized with either ice or isoflurane then fileted and fixed for 30 min in 4% paraformaldehyde at room temperature after the final imaging time point for these experiments. Following fixation, larval filets were rinsed and washed with PBS with 1% Triton-X then incubated for 1 h and 30 min in blocking buffer (PBS/0.5% TritonX/10% Horse Serum). Following blocking, filets were incubated with primary antibodies (Mouse anti-futsch 1:2, rabbit anti-GFP 1:1000) overnight at 4 °C. Following primary antibody incubation, filets were rinsed and then washed in PBS with 0.5% Triton-X 5 times for 10 min each. Filets were then incubated with secondary antibodies (Goat anti-mouse 647 and Goat anti-rabbit 488) overnight at 4 °C. Filets were then rinsed and washed in PBS with 0.5% Triton-X 5 times for 15 min each. Filets were mounted on glass slides with 1:1 1xPBS and Glycerol for later imaging.

Quantification and statistical analysis

Dendrite arbors were traced using the Simple Neurite Tracer plugin in ImageJ to determine the number of dendrite branch tips and the total length of all the dendrite branches. For some neurons, using these traced arbors, Sholl analysis of dendrite branches crossing circles separated by 1 μm was performed. For single branch injury analysis, normalized control neurons were used for comparison. Normalized controls represent uninjured neurons normalized for one less primary dendrite branch by eliminating the least branched primary dendrite branch and its secondary and terminal branches from quantification. For all graphs comparing means, values are plotted as mean ± SEM and individual data points representing individual neurons are shown. For paired data, values are plotted for individual neurons with faded lines connecting repeated measurements at 24 and 72 h after injury. Solid lines represent the slope (m) between the mean 24 and 72 h after injury values which were calculated with the formula $m = \frac{((mean\ at\ 72\ hours\ after\ injury) - (mean\ at\ 24\ hours\ after\ injury))}{72-24}$.

Percent branches gained and percent length gained were calculated with the formula $\%\ Change = ((mean\ at\ 72\ hours\ after\ injury) - (mean\ at\ 24\ hours\ after\ injury)) * 100\%$. For both GMA and TauGFP analysis, mean RFU values for branches were calculated in ImageJ by measuring the mean fluorescence of ~ 50 μm stretches of individual primary branches (starting as close to the cell body as possible) and subtracting local mean background fluorescence around the branch and then calculating the mean RFU of all primary branches taken together. For both GMA and TauGFP analysis, median RFU for neuron cell bodies were calculated in ImageJ by measuring the median fluorescence of the entire cell body and subtracting local median background fluorescence around the cell body. For EB-1 comet analysis, we used the open-source version of the software KymoButler to measure comet velocity[116].

Sample sizes are represented within figures other than the following. Figure 1B: WT 24–168 h AEL n = 21, n = 10, n = 10, n = 17, n = 9, n = 5, n = 10 respectively; ATX1.82Q 24–168 h AEL n = 9, n = 10, n = 10, n = 10, n = 8, n = 9, n = 6 respectively; ATX1.30Q 24,96,168 h AEL n = 6, n = 8, n = 6 respectively; ATX2.64Q 24–168 h AEL n = 10, n = 6, n = 8, n = 11, n = 11, n = 7, n = 10 respectively; ATX2.22Q 24,96,168 h AEL n = 5, n = 6, n = 5 respectively; MJD.78Q 24–168 h AEL n = 10, n = 9, n = 12, n = 7, n = 8, n = 11, n = 10 respectively; MJD.27Q

24,96,168 h AEL n = 6, n = 6, n = 6 respectively; and HTT231NT.128Q 24–168 h AEL n = 12, n = 6, n = 5, n = 5, n = 5, n = 9, n = 7 respectively. Figure 1C, Supp1D, Supp 1C: WT 24–168 h AEL n = 14, n = 10, n = 10, n = 10, n = 9, n = 5, n = 5 respectively; ATX1.82Q 24–168 h AEL n = 9, n = 10, n = 10, n = 10, n = 8, n = 9, n = 6 respectively; ATX2.64Q 24–168 h AEL n = 10, n = 6, n = 8, n = 11, n = 11, n = 7, n = 10 respectively; MJD.78Q 24–168 h AEL n = 10, n = 9, n = 12, n = 7, n = 8, n = 11, n = 10 respectively; and HTT231NT.128Q 24–168 h AEL n = 12, n = 6, n = 5, n = 5, n = 5, n = 9, n = 7 respectively. Figure Supp1B: WT 48 h AEL n = 1, WT 96 h AEL n = 3 WT 120 h AEL n = 2 ATX1.82Q 48 h AEL n = 1, ATX1.82Q 96 h AEL n = 3, ATX1.82Q 120 h AEL n = 2, MJD.78Q 48 h AEL n = 4, MJD.78Q 96 h AEL n = 3, MJD.78Q 120 h AEL n = 2. Figure Supp1G: WT 24–120 h AEL n = 3, n = 3, n = 3, n = 5, n = 15 respectively; MJD.78Q 24–120 h AEL n = 6, n = 4, n = 3, n = 5, n = 7 respectively; ATX1.82Q 120 h AEL n = 15. Figure Supp1H: WT 96–168 h AEL n = 4,n = 4,n = 5,n = 5 respectively; ATX1.82Q 96-168 h AEL n = 3,n = 3,n = 4,n = 6 respectively; MJD.78Q 96–168 h AEL n = 5,n = 5,n = 6,n-6 respectively. Figure Supp5E: WT UI n = 5, WT SBI n = 5, ATX1.82Q UI n = 7, ATX1.82Q SBI n = 7, ATX2.64Q UI n = 6, ATX2.64Q SBI n = 4. All sample sizes for figures showing both individual neurons at 72 h after injury and paired graphs of 24–72 h after injury are analyzing the same neurons and have the same n.

Statistical analysis was performed using Graphpad Prism software and Microsoft Excel software. The statistical details of experiments can be found in the figure legends. Statistical significance was tested using the two-tailed Welch's t-test for all analysis comparing two groups, using paired t-test for all analysis comparing the same neuron at two time points, and using one-way ANOVA with either Dunnett's or Tukey's multiple comparisons correction for analysis comparing more than two groups. For all statistical tests used $^{****}p < 0.0001$, $^{***}p < 0.001$, $^{**}p < 0.01$, $^{*}p < 0.05$, $^{ns}p \geq 0.05$.

Data availability

The datasets generated during and/or analyzed during the current study are available from the lead contact on reasonable request. This paper does not report original code. Any additional information required to reanalyze the data reported in this paper is available from the lead contact upon request.

Received: 9 May 2024; Accepted: 26 September 2024
Published online: 21 October 2024

References

1. Dorostkar, M. M., Zou, C., Blazquez-Llorca, L. & Herms, J. Analyzing dendritic spine pathology in Alzheimer's disease: Problems and opportunities. *Acta Neuropathol.* **130**, 1–19. https://doi.org/10.1007/s00401-015-1449-5 (2015).
2. Clark, H. B. *et al.* Purkinje cell expression of a mutant allele of SCA1 in transgenic mice leads to disparate effects on motor behaviors, followed by a progressive cerebellar dysfunction and histological alterations. *J. Neurosci.* **17**, 7385–7395. https://doi.org/10.1523/JNEUROSCI.17-19-07385.1997 (1997).
3. Fogarty, M. J., Noakes, P. G. & Bellingham, M. C. Motor cortex layer V pyramidal neurons exhibit dendritic regression, spine loss, and increased synaptic excitation in the presymptomatic hSOD1(G93A) mouse model of amyotrophic lateral sclerosis. *J. Neurosci.* **35**, 643–647. https://doi.org/10.1523/jneurosci.3483-14.2015 (2015).
4. Guidetti, P. *et al.* Early degenerative changes in transgenic mice expressing mutant huntingtin involve dendritic abnormalities but no impairment of mitochondrial energy production. *Exp. Neurol.* **169**, 340–350. https://doi.org/10.1006/exnr.2000.7626 (2001).
5. Stephens, B. *et al.* Evidence of a breakdown of corticostriatal connections in Parkinson's disease. *Neuroscience* **132**, 741–754. https://doi.org/10.1016/j.neuroscience.2005.01.007 (2005).
6. Kweon, J. H., Kim, S. & Lee, S. B. The cellular basis of dendrite pathology in neurodegenerative diseases. *BMB Rep.* **50**, 5–11. https://doi.org/10.5483/bmbrep.2017.50.1.131 (2017).
7. Cochran, J. N., Hall, A. M. & Roberson, E. D. The dendritic hypothesis for Alzheimer's disease pathophysiology. *Brain Res. Bull.* **103**, 18–28. https://doi.org/10.1016/j.brainresbull.2013.12.004 (2014).
8. Šišková, Z. *et al.* Dendritic structural degeneration is functionally linked to cellular hyperexcitability in a mouse model of Alzheimer's disease. *Neuron* **84**, 1023–1033. https://doi.org/10.1016/j.neuron.2014.10.024 (2014).
9. Ferrer, I., Kulisevski, J., Vazquez, J., Gonzalez, G. & Pineda, M. Purkinje cells in degenerative diseases of the cerebellum and its connections: A Golgi study. *Clin. Neuropathol.* **7**, 22–28 (1988).
10. Ferrer, I. Neurons and their dendrites in frontotemporal dementia. *Dement. Geriatr. Cogn. Disord.* **10**(Suppl 1), 55–60. https://doi.org/10.1159/000051214 (1999).
11. Chan-Palay, V. & Asan, E. Alterations in catecholamine neurons of the locus coeruleus in senile dementia of the Alzheimer type and in Parkinson's disease with and without dementia and depression. *J. Comp. Neurol.* **287**, 373–392. https://doi.org/10.1002/cne.902870308 (1989).
12. Vagn-Hansen, L., Reske-Nielsen, E. & Lou, H. C. Menkes' disease–a new leucodystrophy (?). A clinical and neuropathological review together with a new case. *Acta Neuropathol.* **25**, 103–119. https://doi.org/10.1007/bf00687555 (1973).
13. Crosby, T. W. & Chou, S. M. "Ragged-red" fibers in Leigh's disease. *Neurology* **24**, 49–54. https://doi.org/10.1212/wnl.24.1.49 (1974).
14. McNeill, T. H., Brown, S. A., Rafols, J. A. & Shoulson, I. Atrophy of medium spiny I striatal dendrites in advanced Parkinson's disease. *Brain Res.* **455**, 148–152. https://doi.org/10.1016/0006-8993(88)90124-2 (1988).
15. Ferrante, R. J., Kowall, N. W. & Richardson, E. P. Proliferative and degenerative changes in striatal spiny neurons in Huntington's disease: A combined study using the section-Golgi method and calbindin D28k immunocytochemistry. *J. Neurosci.* **11**, 3877–3887. https://doi.org/10.1523/jneurosci.11-12-03877.1991 (1991).
16. Hammer, R. P., Tomiyasu, U. & Scheibel, A. B. Degeneration of the human Betz cell due to amyotrophic lateral sclerosis. *Exp. Neurol.* **63**, 336–346. https://doi.org/10.1016/0014-4886(79)90129-8 (1979).
17. Spires, T. L. *et al.* Dendritic spine pathology and deficits in experience-dependent dendritic plasticity in R6/1 Huntington's disease transgenic mice. *Eur. J. Neurosci.* **19**, 2799–2807. https://doi.org/10.1111/j.0953-816x.2004.03374.x (2004).
18. Murmu, R. P., Li, W., Holtmaat, A. & Li, J.-Y. Dendritic spine instability leads to progressive neocortical spine loss in a mouse model of Huntington's disease. *J. Neurosci.* **33**, 12997–13009. https://doi.org/10.1523/jneurosci.5284-12.2013 (2013).
19. Fogarty, M. J., Mu, E. W. H., Lavidis, N. A., Noakes, P. G. & Bellingham, M. C. Motor areas show altered dendritic structure in an amyotrophic lateral sclerosis mouse model. *Front. Neurosci.* **11**, 609. https://doi.org/10.3389/fnins.2017.00609 (2017).
20. Fogarty, M. J., Mu, E. W. H., Noakes, P. G., Lavidis, N. A. & Bellingham, M. C. Marked changes in dendritic structure and spine density precede significant neuronal death in vulnerable cortical pyramidal neuron populations in the SOD1(G93A) mouse model of amyotrophic lateral sclerosis. *Acta Neuropathol. Commun.* **4**, 77. https://doi.org/10.1186/s40478-016-0347-y (2016).

21. Pelaez, M. C. *et al.* Neuronal dysfunction caused by FUSR521G promotes ALS-associated phenotypes that are attenuated by NF-κB inhibition. *Acta Neuropathol. Commun.* **11**, 182. https://doi.org/10.1186/s40478-023-01671-1 (2023).
22. Herms, J. & Dorostkar, M. M. Dendritic spine pathology in neurodegenerative diseases. *Annu. Rev. Pathol.* **11**, 221–250. https://doi.org/10.1146/annurev-pathol-012615-044216 (2016).
23. Thompson-Peer, K. L., DeVault, L., Li, T., Jan, L. Y. & Jan, Y. N. In vivo dendrite regeneration after injury is different from dendrite development. *Genes Dev.* **30**, 1776–1789. https://doi.org/10.1101/gad.282848.116 (2016).
24. Stone, M. C., Albertson, R. M., Chen, L. & Rolls, M. M. Dendrite injury triggers DLK-independent regeneration. *Cell Rep.* **6**, 247–253. https://doi.org/10.1016/j.celrep.2013.12.022 (2014).
25. Song, Y. *et al.* Regeneration of *Drosophila* sensory neuron axons and dendrites is regulated by the Akt pathway involving Pten and microRNA bantam. *Genes Dev.* **26**, 1612–1625. https://doi.org/10.1101/gad.193243.112 (2012).
26. DeVault, L. *et al.* Dendrite regeneration of adult *Drosophila* sensory neurons diminishes with aging and is inhibited by epidermal-derived matrix metalloproteinase 2. *Genes Dev.* **32**, 402–414. https://doi.org/10.1101/gad.308270.117 (2018).
27. Li, M. *et al.* Motor neuron-specific RhoA knockout delays degeneration and promotes regeneration of dendrites in spinal ventral horn after brachial plexus injury. *Neural Regen. Res.* **18**, 2757–2761. https://doi.org/10.4103/1673-5374.373657 (2023).
28. Stone, M. C., Seebold, D. Y., Shorey, M., Kothe, G. O. & Rolls, M. M. Dendrite regeneration in the vertebrate spinal cord. *Dev. Biol.* **488**, 114–119. https://doi.org/10.1016/j.ydbio.2022.05.014 (2022).
29. Agostinone, J. *et al.* Insulin signalling promotes dendrite and synapse regeneration and restores circuit function after axonal injury. *Brain* **141**, 1963–1980. https://doi.org/10.1093/brain/awy142(2018).
30. Ji, Y. *et al.* Poststroke dendritic arbor regrowth requires the actin nucleator Cobl. *PLoS Biol.* **19**, e3001399. https://doi.org/10.1371/journal.pbio.3001399 (2021).
31. Grueber, W. B., Jan, L. Y. & Jan, Y. N. Tiling of the *Drosophila* epidermis by multidendritic sensory neurons. *Development* **129**, 2867–2878. https://doi.org/10.1242/dev.129.12.2867 (2002).
32. Bonini, N. M. A perspective on *Drosophila* genetics and its insight into human neurodegenerative disease. *Front. Mol. Biosci.* **9**, 1060796. https://doi.org/10.3389/fmolb.2022.1060796 (2022).
33. Lu, B. Recent advances in using *Drosophila* to model neurodegenerative diseases. *Apoptosis* **14**, 1008–1020. https://doi.org/10.1007/s10495-009-0347-5 (2009).
34. Lu, B. & Vogel, H. Drosophila models of neurodegenerative diseases. *Annu. Rev. Pathol.* **4**, 315–342. https://doi.org/10.1146/annurev.pathol.3.121806.151529 (2009).
35. Koon, A. C. & Chan, H. Y. E. *Drosophila* melanogaster as a model organism to study RNA toxicity of repeat expansion-associated neurodegenerative and neuromuscular diseases. *Front. Cell. Neurosci.* **11**, 70. https://doi.org/10.3389/fncel.2017.00070 (2017).
36. Lessing, D. & Bonini, N. M. Maintaining the brain: Insight into human neurodegeneration from *Drosophila* melanogaster mutants. *Nat. Rev. Genet.* **10**, 359–370. https://doi.org/10.1038/nrg2563 (2009).
37. Al-Ramahi, I. *et al.* High-throughput Functional analysis distinguishes pathogenic, nonpathogenic, and compensatory transcriptional changes in neurodegeneration. *Cell Syst.* **7**, 28-40.e4. https://doi.org/10.1016/j.cels.2018.05.010 (2018).
38. Xiong, Y. & Yu, J. Modeling Parkinson's disease in drosophila: What have we learned for dominant traits?. *Front. Neurol.* **9**, 228. https://doi.org/10.3389/fneur.2018.00228 (2018).
39. Prüßing, K., Voigt, A. & Schulz, J. B. Drosophila melanogaster as a model organism for Alzheimer's disease. *Mol. Neurodegener.* **8**, 35. https://doi.org/10.1186/1750-1326-8-35 (2013).
40. Tandon, S., Aggarwal, P. & Sarkar, S. Polyglutamine disorders: Pathogenesis and potential drug interventions. *Life Sci.* **344**, 122562. https://doi.org/10.1016/j.lfs.2024.122562 (2024).
41. Warrick, J. M. *et al.* Expanded polyglutamine protein forms nuclear inclusions and causes neural degeneration in *Drosophila*. *Cell* **93**, 939–949. https://doi.org/10.1016/s0092-8674(00)81200-3 (1998).
42. Jackson, G. R. *et al.* Polyglutamine-expanded human huntingtin transgenes induce degeneration of *Drosophila* photoreceptor neurons. *Neuron* **21**, 633–642. https://doi.org/10.1016/s0896-6273(00)80573-5 (1998).
43. Barwell, T., Raina, S., Page, A., MacCharles, H. & Seroude, L. Juvenile and adult expression of polyglutamine expanded huntingtin produce distinct aggregate distributions in *Drosophila* muscle. *Hum. Mol. Genet.* **32**(16), 2656–2668. https://doi.org/10.1093/hmg/ddad098 (2023).
44. Fernandez-Funez, P. *et al.* Identification of genes that modify ataxin-1-induced neurodegeneration. *Nature* **408**, 101–106. https://doi.org/10.1038/35040584 (2000).
45. Lee, S. B., Bagley, J. A., Lee, H. Y., Jan, L. Y. & Jan, Y.-N. Pathogenic polyglutamine proteins cause dendrite defects associated with specific actin cytoskeletal alterations in Drosophila. *Proc. Natl. Acad. Sci. U.S.A.* **108**, 16795–16800. https://doi.org/10.1073/pnas.1113573108 (2011).
46. Kretzschmar, D. *et al.* Glial and neuronal expression of polyglutamine proteins induce behavioral changes and aggregate formation in *Drosophila*. *Glia* **49**, 59–72. https://doi.org/10.1002/glia.20098 (2005).
47. Lee, W.-C.M., Yoshihara, M. & Littleton, J. T. Cytoplasmic aggregates trap polyglutamine-containing proteins and block axonal transport in a *Drosophila* model of Huntington's disease. *Proc. Natl. Acad. Sci. U.S.A.* **101**, 3224–3229. https://doi.org/10.1073/pnas.0400243101 (2004).
48. Warrick, J. M. *et al.* Suppression of polyglutamine-mediated neurodegeneration in *Drosophila* by the molecular chaperone HSP70. *Nat. Genet.* **23**, 425–428. https://doi.org/10.1038/70532 (1999).
49. Kim, Y.-T., Shin, S. M., Lee, W. Y., Kim, G.-M. & Jin, D. K. Expression of expanded polyglutamine protein induces behavioral changes in Drosophila (polyglutamine-induced changes in *Drosophila*). *Cell. Mol. Neurobiol.* **24**, 109–122. https://doi.org/10.1023/b:cemn.0000012716.14075.25 (2004).
50. McGurk, L. *et al.* Toxicity of pathogenic ataxin-2 in *Drosophila* shows dependence on a pure CAG repeat sequence. *Hum. Mol. Genet.* **30**(19), 1797–1810. https://doi.org/10.1093/hmg/ddab148 (2021).
51. Li, L.-B., Yu, Z., Teng, X. & Bonini, N. M. RNA toxicity is a component of ataxin-3 degeneration in *Drosophila*. *Nature* **453**, 1107–1111. https://doi.org/10.1038/nature06909 (2008).
52. Branco, J. *et al.* Comparative analysis of genetic modifiers in Drosophila points to common and distinct mechanisms of pathogenesis among polyglutamine diseases. *Hum. Mol. Genet.* **17**, 376–390. https://doi.org/10.1093/hmg/ddm315 (2008).
53. Tsou, W.-L. *et al.* Ubiquitination regulates the neuroprotective function of the deubiquitinase ataxin-3 in vivo. *J. Biol. Chem.* **288**, 34460–34469. https://doi.org/10.1074/jbc.m113.513903 (2013).
54. Kim, H.-J. *et al.* Therapeutic modulation of eIF2α phosphorylation rescues TDP-43 toxicity in amyotrophic lateral sclerosis disease models. *Nat. Genet.* **46**, 152–160. https://doi.org/10.1038/ng.2853 (2014).
55. Bonini, N. Bonini insertions. *FlyBase*. http://flybase.org/reports/FBrf0178823.htm (2004).
56. Molero, A. E. *et al.* Selective expression of mutant huntingtin during development recapitulates characteristic features of Huntington's disease. *Proc. Natl. Acad. Sci. U.S.A.* **113**, 5736–5741. https://doi.org/10.1073/pnas.1603871113 (2016).
57. Serra, H. G. *et al.* RORalpha-mediated Purkinje cell development determines disease severity in adult SCA1 mice. *Cell* **127**, 697–708. https://doi.org/10.1016/j.cell.2006.09.036 (2006).
58. Tereshchenko, A. V. *et al.* Abnormal development of cerebellar-striatal circuitry in Huntington disease. *Neurology* **94**, e1908–e1915. https://doi.org/10.1212/wnl.0000000000009364 (2020).
59. van der Plas, E., Schultz, J. L. & Nopoulos, P. C. The neurodevelopmental hypothesis of Huntington's disease. *J. Huntingtons Dis.* **9**, 217–229. https://doi.org/10.3233/jhd-200394(2020).

60. Wennagel, D., Braz, B. Y. & Humbert, S. Treating early transient neuronal defects in a mouse model of Huntington's disease delays the signs of the disease in adulthood. *Med. Sci. (Paris)* **39**, 313–316. https://doi.org/10.1051/medsci/2023036 (2023).
61. Capizzi, M. *et al.* Developmental defects in Huntington's disease show that axonal growth and microtubule reorganization require NUMA1. *Neuron* **110**, 36-50.e5. https://doi.org/10.1016/j.neuron.2021.10.033 (2022).
62. Barnat, M. *et al.* Huntington's disease alters human neurodevelopment. *Science* **369**, 787–793. https://doi.org/10.1126/science.aax3338 (2020).
63. Fieguin, F. UAS-hMAPT constructs and insertions from Fabian Feiguin. *FlyBase*. http://flybase.org/reports/FBrf0252283.htm (2021).
64. Stone, M. C., Nguyen, M. M., Tao, J., Allender, D. L. & Rolls, M. M. Global up-regulation of microtubule dynamics and polarity reversal during regeneration of an axon from a dendrite. *Mol. Biol. Cell* **21**, 767–777. https://doi.org/10.1091/mbc.e09-11-0967 (2010).
65. Bradke, F. & Dotti, C. G. Differentiated neurons retain the capacity to generate axons from dendrites. *Curr. Biol.* **10**, 1467–1470. https://doi.org/10.1016/s0960-9822(00)00807-1 (2000).
66. Gomis-Rüth, S., Wierenga, C. J. & Bradke, F. Plasticity of polarization: Changing dendrites into axons in neurons integrated in neuronal circuits. *Curr. Biol.* **18**, 992–1000. https://doi.org/10.1016/j.cub.2008.06.026 (2008).
67. Dutta, D., Bloor, J. W., Ruiz-Gomez, M., VijayRaghavan, K. & Kiehart, D. P. Real-time imaging of morphogenetic movements in Drosophila using Gal4-UAS-driven expression of GFP fused to the actin-binding domain of moesin. *Genesis* **34**, 146–151. https://doi.org/10.1002/gene.10113 (2002).
68. Edwards, K. A., Demsky, M., Montague, R. A., Weymouth, N. & Kiehart, D. P. GFP-moesin illuminates actin cytoskeleton dynamics in living tissue and demonstrates cell shape changes during morphogenesis in Drosophila. *Dev. Biol.* **191**, 103–117. https://doi.org/10.1006/dbio.1997.8707 (1997).
69. Kilo, L., Stürner, T., Tavosanis, G. & Ziegler, A. B. Drosophila dendritic arborisation neurons: Fantastic actin dynamics and where to find them. *Cells* **10**, 2777. https://doi.org/10.3390/cells10102777 (2021).
70. Rolls, M. M. *et al.* Polarity and intracellular compartmentalization of Drosophila neurons. *Neural Dev.* **2**, 7. https://doi.org/10.1186/1749-8104-2-7 (2007).
71. Stone, M. C., Roegiers, F. & Rolls, M. M. Microtubules have opposite orientation in axons and dendrites of *Drosophila* neurons. *Mol. Biol. Cell* **19**, 4122–4129. https://doi.org/10.1091/mbc.e07-10-1079 (2008).
72. Clyne, P. J., Brotman, J. S., Sweeney, S. T. & Davis, G. Green fluorescent protein tagging *Drosophila* proteins at their native genomic loci with small P elements. *Genetics* **165**, 1433–1441. https://doi.org/10.1093/genetics/165.3.1433 (2003).
73. Nanda, S., Bhattacharjee, S., Cox, D. N. & Ascoli, G. A. Distinct relations of microtubules and actin filaments with dendritic architecture. *iScience* **23**, 101865. https://doi.org/10.1016/j.isci.2020.101865 (2020).
74. Brar, H. K. *et al.* Dendrite regeneration in *C. elegans* is controlled by the RAC GTPase CED-10 and the RhoGEF TIAM-1. *PLoS Genet.* **18**, e1010127. https://doi.org/10.1371/journal.pgen.1010127 (2022).
75. Feng, C. *et al.* Patronin-mediated minus end growth is required for dendritic microtubule polarity. *J. Cell Biol.* **218**, 2309–2328. https://doi.org/10.1083/jcb.201810155 (2019).
76. Hertzler, J. I. *et al.* Kinetochore proteins suppress neuronal microtubule dynamics and promote dendrite regeneration. *Mol. Biol. Cell* **31**, 2125–2138. https://doi.org/10.1091/mbc.e20-04-0237-t (2020).
77. Nye, D. M. R. *et al.* The receptor tyrosine kinase Ror is required for dendrite regeneration in *Drosophila* neurons. *PLoS Biol.* **18**, e3000657. https://doi.org/10.1371/journal.pbio.3000657 (2020).
78. Brunden, K. R., Lee, V.M.-Y., Smith, A. B., Trojanowski, J. Q. & Ballatore, C. Altered microtubule dynamics in neurodegenerative disease: Therapeutic potential of microtubule-stabilizing drugs. *Neurobiol. Dis.* **105**, 328–335. https://doi.org/10.1016/j.nbd.2016.12.021 (2017).
79. Sferra, A., Nicita, F. & Bertini, E. Microtubule dysfunction: A common feature of neurodegenerative diseases. *Int. J. Mol. Sci.* **21**, 7354. https://doi.org/10.3390/ijms21197354 (2020).
80. Cyske, Z., Gaffke, L., Pierzynowska, K. & Węgrzyn, G. Tubulin cytoskeleton in neurodegenerative diseases-not only primary tubulinopathies. *Cell. Mol. Neurobiol.* **43**, 1867–1884. https://doi.org/10.1007/s10571-022-01304-6 (2023).
81. Wurz, A. I., Schulz, A. M., O'Bryant, C. T., Sharp, J. F. & Hughes, R. M. Cytoskeletal dysregulation and neurodegenerative disease: Formation, monitoring, and inhibition of cofilin-actin rods. *Front. Cell. Neurosci.* **16**, 982074. https://doi.org/10.3389/fncel.2022.982074 (2022).
82. Muñoz-Lasso, D. C., Romá-Mateo, C., Pallardó, F. V. & Gonzalez-Cabo, P. Much more than a scaffold: cytoskeletal proteins in neurological disorders. *Cells* **9**, 358. https://doi.org/10.3390/cells9020358 (2020).
83. McMurray, C. T. Neurodegeneration: Diseases of the cytoskeleton?. *Cell Death Differ.* **7**, 861–865. https://doi.org/10.1038/sj.cdd.4400764 (2000).
84. Sen, S., Lagas, S., Roy, A. & Kumar, H. Cytoskeleton saga: Its regulation in normal physiology and modulation in neurodegenerative disorders. *Eur. J. Pharmacol.* **925**, 175001. https://doi.org/10.1016/j.ejphar.2022.175001 (2022).
85. Martín-Cámara, O., Cores, Á., López-Alvarado, P. & Menéndez, J. C. Emerging targets in drug discovery against neurodegenerative diseases: Control of synapsis disfunction by the RhoA/ROCK pathway. *Eur. J. Med. Chem.* **225**, 113742. https://doi.org/10.1016/j.ejmech.2021.113742 (2021).
86. Shehjar, F., Almarghalani, D. A., Mahajan, R., Hasan, S.A.-M. & Shah, Z. A. The multifaceted role of cofilin in neurodegeneration and stroke: insights into pathogenesis and targeting as a therapy. *Cells* **13**, 188. https://doi.org/10.3390/cells13020188 (2024).
87. Gutiérrez-Vargas, J. A., Castro-Álvarez, J. F., Zapata-Berruecos, J. F., Abdul-Rahim, K. & Arteaga-Noriega, A. Neurodegeneration and convergent factors contributing to the deterioration of the cytoskeleton in Alzheimer's disease, cerebral ischemia and multiple sclerosis (Review). *Biomed. Rep.* **16**, 27. https://doi.org/10.3892/br.2022.1510 (2022).
88. Eira, J., Silva, C. S., Sousa, M. M. & Liz, M. A. The cytoskeleton as a novel therapeutic target for old neurodegenerative disorders. *Prog. Neurobiol.* **141**, 61–82. https://doi.org/10.1016/j.pneurobio.2016.04.007 (2016).
89. Hao, Y. *et al.* An evolutionarily conserved mechanism for cAMP elicited axonal regeneration involves direct activation of the dual leucine zipper kinase DLK. *eLife* **5**, e14048. https://doi.org/10.7554/eLife.14048 (2016).
90. Nix, P. & Bastiani, M. DLK: The "preconditioning" signal for axon regeneration?. *Neuron* **74**, 961–963. https://doi.org/10.1016/j.neuron.2012.06.005 (2012).
91. Shin, J. E. *et al.* Dual leucine zipper kinase is required for retrograde injury signaling and axonal regeneration. *Neuron* **74**, 1015–1022. https://doi.org/10.1016/j.neuron.2012.04.028 (2012).
92. Yan, D., Wu, Z., Chisholm, A. D. & Jin, Y. The DLK-1 kinase promotes mRNA stability and local translation in *C. elegans* synapses and axon regeneration. *Cell* **138**, 1005–1018. https://doi.org/10.1016/j.cell.2009.06.023 (2009).
93. Ghosh-Roy, A., Wu, Z., Goncharov, A., Jin, Y. & Chisholm, A. D. Calcium and cyclic AMP promote axonal regeneration in *Caenorhabditis elegans* and require DLK-1 kinase. *J. Neurosci.* **30**, 3175–3183. https://doi.org/10.1523/jneurosci.5464-09.2010 (2010).
94. Emoto, K. Signaling mechanisms that coordinate the development and maintenance of dendritic fields. *Curr. Opin. Neurobiol.* **22**, 805–811. https://doi.org/10.1016/j.conb.2012.04.005 (2012).
95. Lin, Y.-C. & Koleske, A. J. Mechanisms of synapse and dendrite maintenance and their disruption in psychiatric and neurodegenerative disorders. *Annu. Rev. Neurosci.* **33**, 349–378. https://doi.org/10.1146/annurev-neuro-060909-153204 (2010).
96. Koleske, A. J. Molecular mechanisms of dendrite stability. *Nat. Rev. Neurosci.* **14**, 536–550. https://doi.org/10.1038/nrn3486 (2013).

97. Neumann, S., Skinner, K. & Basbaum, A. I. Sustaining intrinsic growth capacity of adult neurons promotes spinal cord regeneration. *Proc. Natl. Acad. Sci. U.S.A.* **102**, 16848–16852. https://doi.org/10.1073/pnas.0508538102 (2005).
98. Kirby, E. D. *et al.* Acute stress enhances adult rat hippocampal neurogenesis and activation of newborn neurons via secreted astrocytic FGF2. *eLife* **2**, e00362. https://doi.org/10.7554/elife.00362 (2013).
99. Becker, F., Behrends, M. M. & Rudolph, K. L. Evolution, mechanism and limits of dietary restriction induced health benefits & longevity. *Redox Biol.* **63**, 102725. https://doi.org/10.1016/j.redox.2023.102725 (2023).
100. Green, C. L., Lamming, D. W. & Fontana, L. Molecular mechanisms of dietary restriction promoting health and longevity. *Nat. Rev. Mol. Cell Biol.* **23**, 56–73. https://doi.org/10.1038/s41580-021-00411-4 (2022).
101. Zhang, L. *et al.* Beneficial effects on brain micro-environment by caloric restriction in alleviating neurodegenerative diseases and brain aging. *Front. Physiol.* **12**, 715443. https://doi.org/10.3389/fphys.2021.715443 (2021).
102. Krzyzosiak, A. *et al.* Target-based discovery of an inhibitor of the regulatory phosphatase PPP1R15B. *Cell* **174**, 1216-1228.e19. https://doi.org/10.1016/j.cell.2018.06.030 (2018).
103. Derisbourg, M. J., Hartman, M. D. & Denzel, M. S. Perspective: Modulating the integrated stress response to slow aging and ameliorate age-related pathology. *Nat. Aging* **1**, 760–768. https://doi.org/10.1038/s43587-021-00112-9 (2021).
104. Colla, E. *et al.* Accumulation of toxic α-synuclein oligomer within endoplasmic reticulum occurs in α-synucleinopathy in vivo. *J. Neurosci.* **32**, 3301–3305. https://doi.org/10.1523/jneurosci.5368-11.2012 (2012).
105. Wang, L., Popko, B. & Roos, R. P. An enhanced integrated stress response ameliorates mutant SOD1-induced ALS. *Hum. Mol. Genet.* **23**, 2629–2638. https://doi.org/10.1093/hmg/ddt658 (2014).
106. Schor, N. F. & Bianchi, D. W. Neurodevelopmental clues to neurodegeneration. *Pediatr. Neurol.* **123**, 67–76. https://doi.org/10.1016/j.pediatrneurol.2021.07.012 (2021).
107. Shabani, K. & Hassan, B. A. The brain on time: Links between development and neurodegeneration. *Development* **10**, dev200397. https://doi.org/10.1242/dev.200397 (2023).
108. Grice, S. J. & Liu, J.-L. Neurodevelopmental defects as a primer of neurodegeneration: lessons from spinal muscular atrophy and Huntington's disease. *Neural Regen. Res.* **18**, 1952–1953. https://doi.org/10.4103/1673-5374.367844 (2023).
109. Han, C., Jan, L. Y. & Jan, Y.-N. Enhancer-driven membrane markers for analysis of nonautonomous mechanisms reveal neuron-glia interactions in Drosophila. *Proc. Natl. Acad. Sci. U.S.A.* **108**, 9673–9678. https://doi.org/10.1073/pnas.1106386108 (2011).
110. Grueber, W. B., Jan, L. Y. & Jan, Y. N. Different levels of the homeodomain protein cut regulate distinct dendrite branching patterns of Drosophila multidendritic neurons. *Cell* **112**, 805–818. https://doi.org/10.1016/s0092-8674(03)00160-0 (2003).
111. Cheng, L. E., Song, W., Looger, L. L., Jan, L. Y. & Jan, Y. N. The role of the TRP channel NompC in Drosophila larval and adult locomotion. *Neuron* **67**, 373–380. https://doi.org/10.1016/j.neuron.2010.07.004 (2010).
112. Kiehart, D. UAS-Moe.GFP insertions. http://flybase.org/reports/FBrf0211536.htm (2010).
113. Scholey, J. P{UAS-EB1-GFP}3. http://flybase.org/reports/FBrf0213553.htm (2011).
114. Rumpf, S., Lee, S. B., Jan, L. Y. & Jan, Y. N. Neuronal remodeling and apoptosis require VCP-dependent degradation of the apoptosis inhibitor DIAP1. *Development* **138**, 1153–1160. https://doi.org/10.1242/dev.062703 (2011).
115. Rao, K. S. & Rolls, M. M. Two Drosophila model neurons can regenerate axons from the stump or from a converted dendrite, with feedback between the two sites. *Neural Dev.* **12**, 15. https://doi.org/10.1186/s13064-017-0092-3 (2017).
116. Jakobs, M. A. H., Dimitracopoulos, A. & Franze, K. KymoButler, a deep learning software for automated kymograph analysis. *eLife* **8**, e42288. https://doi.org/10.7554/eLife.42288 (2019).

Acknowledgements

Research in this publication was supported by NIH Grant R00NS097627 (to KTP). Research reported in this publication was also supported by the California Institute for Regenerative Medicine under Award Number EDUC4-12822. The content is solely the responsibility of the authors and does not necessarily represent the official views of the California Institute for Regenerative Medicine. The authors would also like to acknowledge the University of California Irvine's Undergraduate Research Opportunities Program and Summer Undergraduate Research Program (UROP and SURP). We thank Vicky Lam for other informative data analysis work not included here. We thank Vinicius Duarte, Rosty Brichko, Mia Brantley, and Yuting Liu for their intellectual contributions to this work. We thank Nancy Bonini, Juan Botas, and Melissa Rolls for providing certain *Drosophila* stocks. Schematics in figures 2, 3, 4, and S3 were created with BioRender.com. We thank the UCI Optical Biology Core and Dr. Adeela Syed for extensive use of the microscopes in their facility. This study was made possible in part through access to the Optical Biology Core Facility of the Developmental Biology Center, a shared resource supported by the Cancer Center Support Grant (CA-62203), the Center for Complex Biological Systems Support Grant (GM-076516), and NIH-S10OD032327 at the University of California, Irvine. KTP is a fellow of the Hellman Foundation.

Author contributions

Conceptualization, S.E.P. and K.T.P.; Methodology, S.E.P. and K.T.P.; Formal Analysis, S.E.P., I.N.B., D.S., G.E.J., A.M., L.U.D, H.H.N.L.; Investigation, S.E.P., I.N.B., D.S., P.T.H., J.G.M.; Resources, K.T.P.; Data Curation, S.E.P.; Writing—Original Draft, S.E.P. and K.T.P; Writing—Review and Editing, S.E.P., P.T.H., K.T.P.; Visualization, S.E.P.; Supervision, K.T.P.; Project Administration, S.E.P., K.T.P.; Funding Acquisition, S.E.P., K.T.P., I.N.B., D.S., A.M., L.U.D.

Additional information

Supplementary Information The online version contains supplementary material available at https://doi.org/10.1038/s41598-024-74670-4.

Correspondence and requests for materials should be addressed to K.L.T.-P.